

## Validated Three Dimensional Unsteady Finite Element Environmental Model, SUITE-3D, for Advection-Diffusion Flows and Air Pollution

Youssef I. Hafez

Independent Researcher, Professor Emeritus, Nile Research Institute, Egypt

Received 30 December 2021; Accepted 20 June 2022

### Abstract

A three dimensional unsteady finite element environmental model, SUITE-3D (Solving Unsteady Incompressible Transport Equation in Three Dimensions, 3D), is developed to solve the advection-diffusion transport equation with decay and source terms. Since there is no general analytical solution to the full advection-diffusion transport equation under all possible boundary conditions and under the different equation parameters, an additional model such as SUITE-3D will aid in giving more insights into the phenomenon of advection-diffusion and pollutant transport. It is important to investigate air pollution modelling in the era of climate change and global warming, that our planet earth is facing nowadays. SUITE-3D uses the standard Galerkin's method without upwinding. Difference schemes are used (central, backward, forward) for the time integration. The finite elements are 8-node cubic brick elements (hexahedrons). Eight Gaussian quadrature points are used for the numerical integration of the element matrices. SUITE-3D is validated against exact solutions of two problems; one has only advection and diffusion terms while the other has advection-diffusion-decay-source terms. The total percentage relative error for the first case was less than 0.61% while it reached 1.0% in the second case. The model is applied to study air pollution dispersion due to a point source pollutant. It is noted that neglecting the x-diffusion term in the Gaussian plume model under calm wind conditions (velocity = 0.2 m/s) results in under-prediction of concentration by 81% at 180 m downstream of the pollutant source. This proves that Gaussian models such as AERMOD provide poor results in situations with low wind speeds, where the three-dimensional diffusion is significant.

*Keywords:* Three dimensional (3D); Environmental flows, unsteady; advection-diffusion-decay-source; Finite Element Method; Air pollution modeling; Gaussian plume models, AERMOD model

### 1. Introduction

The transport phenomenon has been recognized for its importance in many environmental engineering, applied mathematics, and applied science applications. Mass and heat are just few examples of basic quantities that their transport in solids, fluids and gases (especially air and water), have been investigated in great details. Such investigations are facilitated by the existence of mathematical description of the transport phenomenon via the advection and diffusion (AD) differential equation (Eq. (1) hereinafter) and the progress in computational power via high-speed computers. The transport of pollutants in the air constitutes an environmental challenge as far as assessing their magnitude and consequences. The continuous release of pollutants into the open air stresses the importance of air pollution modeling in the era of climate change and global warming, that our planet earth is facing nowadays. Assessing the level of pollution in the air is necessary for environmental health improvement plans and environmental licences permitting for industrial pollution sources.

The unsteady/steady advection-diffusion transport equation has long been solved on different dimensional scales and levels ranging from the one-dimensional, 1D, (e.g. [1], [2]), to two dimensions, 2D, (e.g. [3], [4], [5], [6], [7], [8]) to three dimensions, 3D, (e.g. [9], [10], [11], [12],

[13], [14], [15]).

Hafez and Awad solved the AD equation with the inclusion of a decay term to simulate Radon gas transport in soils. They used the Finite Element Method (FEM) and validated their model with an analytical solution for the AD equation including decay and generation terms with all the coefficients in the transport equations vary as polynomials. Then they verified their model by field data from Greece of Radon transport in soils with multi-layer behaviour where each layer has its own diffusion coefficient. They used a convective-type boundary condition at the soil-air interface where the Radon flux depends on the Radon concentration difference between the ambient air and the soil surface [1].

Svoboda, Z., investigated the combined heat transfer through the building constructions caused by conduction and convection using the finite element method in two dimensions [3]. The FE model was validated with a 1D analytical solution. It was concluded that the lightweight constructions insulated with permeable mineral wool are very sensitive to the convective heat transfer.

Talaa A.M., et al investigated in 2D thermal side discharge into a main channel using the finite element method [4]. To obtain the advective velocities required in the advection-diffusion equation for the temperature transport equation they solved the 2D Navier stokes equations but with a constant turbulent viscosity. They validated both of the hydrodynamic and transport models with experimental data.

\*E-mail address: youssefhafez995@gmail.com

ISSN: 1791-2377 © 2022 School of Science, IHU. All rights reserved.

doi:10.25103/jestr.153.12

Jha, B.K et al studied the calcium profile in the form of 2D advection diffusion equation [5]. A mathematical model is developed that incorporates the important physiological parameters like the diffusion coefficient. Analytic solution was found using Laplace transform in the form of the complementary error function. MATLAB 7.5 has been used to simulate the model and obtain the results.

In 1D models, it is assumed that the variables vary along a longitudinal axis (usually called the x axis) while assuming that all variables are uniform along the z-y plane that is normal to the x axis. In 2D models, the variables are assumed to be changing in a two-dimensional plane (X-Y, or X-Z, or Y-Z) while constancy of the variables are assumed in the third dimension. The requirements of 1D and 2D are due often to: avoiding complexities in model formulation if 3D modelling is used, simplicity of representing the 1D and 2D domains compared to 3D domains, and saving in the computer CPU running time. While 1D and 2D applications of the advection-diffusion transport equations are useful for the application problems to which they are applied, a 3D formulation is of course more general, more accurate, and more representative of the phenomenon at hand.

Gupta, M.M., and Zhang, J., presented an explicit fourth-order compact finite difference scheme for approximating the three-dimensional (3D) convection-diffusion equation with variable coefficients using 19-point formula defined on a uniform cubic grid [9]. They designed a parallelization-oriented multigrid method for fast solution of the resulting linear system. Numerical experiments on a 16 processor vector computer are used to test the high accuracy of the discretization scheme as well as the fast convergence and the parallelization or vectorization efficiency of the solution method. Several test problems are solved and highly accurate solutions of the 3D convection-diffusion equations are obtained for small to medium values of the grid Reynolds number.

Saqib, M, et al developed an efficient numerical scheme for three-dimensional advection-diffusion equation, higher order Alternating Direction Implicit (ADI) method was proposed. Second and fourth order ADI schemes were used to handle such problem [10]. Von Neumann stability analysis shows that Alternating Direction Implicit scheme is unconditionally stable. Their numerical results show that the proposed fourth-order-compact finite-difference scheme is more efficient and produces more accurate results than the second order finite difference scheme while both finite difference schemes are unconditionally stable and highly accurate. Fourth order ADI method was found to be very efficient and stable for solving three-dimensional advection-diffusion equation.

Cheng, H. and Zheng, G. used the Improved Element-Free Galerkin (IEFG) method for solving 3D advection-diffusion problems [11]. The Improved Moving Least-Squares (IMLS) approximation is used to form the trial function; the penalty method is applied to enforce the essential boundary conditions; the Galerkin weak form and the difference method are used to obtain the final discretized equations; and then the formulae of the IEFG method for 3D advection-diffusion problems are presented. The numerical results show that the IEFG method not only has a higher computational speed but also can avoid singular matrix of the Element-Free Galerkin (EFG) method.

An important environmental application of the advection-diffusion transport equation is the transport of pollutants in air. Extensive number of models for solving the transport equation of advection-diffusion exists in the case

of studying air pollution dispersion as seen in the reviews of [16], [17], and [18].

Daly, A. and P. Zannetti in their review report about two important air dispersion models, namely AERMOD and CALPUFF [16]. They stated that AERMOD is a steady-state Gaussian plume model. It uses a single wind field to transport emitted species. The wind field is derived from surface, upper-air, and onsite meteorological observations. AERMOD also combines geophysical data such as terrain elevations and land use with the meteorological data to derive boundary layer parameters such as Monin-Obukhov length, mixing height, stability class, turbulence, etc.

Gaussian models such as AERMOD have an extremely fast response time, because they only calculate a single formula (Eq. (10) hereinafter or similar version of it) for each receptor point instead of solving differential equations. This calculation is almost immediate even on common computers however, meteorological data pre-processing and sophisticated turbulence parameterizations can increase the computational cost, [17].

Gaussian models provide poor results in situations with low wind speeds, where the three-dimensional diffusion is significant. Unfortunately, these situations have proven to be the most dangerous ones in real-life atmospheric dispersion problems as they are often connected to a stably stratified atmosphere or low-level inversions, [19].

Daly, A. and P. Zannetti also reported that CALPUFF is a non-steady state Lagrangian puff dispersion model [16]. The advantage of this model over a Gaussian-based model is that it can realistically simulate the transport of substances in calm, stagnant conditions, complex terrain, and coastal regions with sea/land breezes. CALPUFF is particularly recommended for long-range simulations (e.g., more than 50 miles) and studies involving the assessment of the visual impact of plumes. With the development of the VISTAS Version 6 model2, CALPUFF can use sub-hourly meteorological data and run with sub-hourly time steps. This version of CALPUFF is appropriate for both long-range and short-range simulations, [16].

Puff models such as CALPUFF model show similarities with both Gaussian and Lagrangian dispersion models. They treat the pollution as a superposition of several clouds, "puffs" with a given volume, and calculate the trajectories of these puffs. Puff models separate the model physics by scale: the subpuff scale processes are treated with Gaussian approach (such as by Eq. (10) hereinafter), while above the puff size, Lagrangian trajectories are calculated. The result is a Gaussian plume transported along a wind-driven trajectory instead of a straight centerline as in the standard Gaussian approach. The final concentration field is given as a superposition of the concentration field of each puff. With this two-way approach, puff models can handle spatial and temporal changes of wind direction with keeping the computational cost reasonably low, [17].

Anikender Kumar, P. Goyal obtained an analytical solution of the advection-diffusion equation with the Neumann (total reflection) boundary conditions for a bounded domain for point sources using the separation of variable and wind speed as a power law profile of vertical height above the ground [20]. The analytical model is evaluated with observed concentration at different locations in Delhi, India, which show that the model is performing within a factor of two with observation.

Another research team used AERMOD air quality model to estimate the air pollutant levels of a selected city – Nakhon Ratchasima Municipality, Thailand. Four pollutants

were studied: PM10, CO, SO<sub>2</sub>, and NO<sub>x</sub> [21]. The values of NO<sub>x</sub>, SO<sub>2</sub>, PM10 and CO from AERMOD were 77.88%, 10.59%, 8.98% and 4.14% of those measured at the station, respectively. They attributed the reason that the model's estimation was lower than the actual measurement may be due to pollutant sources which are unaccounted for, such as dust-resuspension from traffic and ground surfaces and other non-point sources.

A group studied the dispersion of two pollutants, namely CO (carbon monoxide) and SO<sub>2</sub> (sulfur dioxide) released from District 7 of Tehran Municipality, Iran, from 20 main line sources, by means of CALPUFF modelling system [22]. CALPUFF is a non-steady state puff modelling software which employs meteorological, terrain, and land-use data to effectively simulate air pollutants' dispersion from a given source. CALMET software has been applied to provide meteorological conditions within the study domain. The simulated hourly mean concentrations of the SO<sub>2</sub> and CO did not follow similar temporal patterns for measurement values. For the absolute value, model results seem to be highly underestimated, compared to the monitored data ( $R^2 = -0.41$ ).

However contrary to the last two cases, [23] investigated the concentrations of SO<sub>2</sub>, NO<sub>x</sub>, and PM<sub>2.5</sub> emitted by 31 brick and tile enterprises in Xinmi City in Zhengzhou China using the CALPUFF model (California puff model, USEPA), they found that the correlation coefficient of the fit curve between the pollutant observed data and the simulated data was higher than 0.8.

The foregoing review indicates that a perfect model is far from being reached and that the needs for development of new models still exist. Since there is no general analytical solution to the full advection-diffusion transport equation under all possible boundary conditions and under the different equation parameters, then an additional model will aid in giving more insights into the phenomenon of air pollution dispersion and modeling. A three dimensional unsteady finite element environmental model, SUITE-3D (Solving Unsteady Incompressible Transport Equation in Three Dimensions, 3D), is developed to solve the advection-diffusion transport equation with decay and source terms. It is hoped that SUITE-3D will shed some light on this highly important environmental topic. SUITE-3D could be a useful tool in testing the accuracy and speed of other similar 3D unsteady models. In the following is a description of SUITE-3D model structure followed by applications to cases that have analytical solutions. Comparison is then made of SUITE-3D with Gaussian air dispersion model under calm wind conditions to highlight the importance of full inclusion of all the transport components or mechanisms such as the downwind diffusion.

## 2. Governing equation and the Finite Element numerical model

The transport process of a substance such as an air pollutant mass can be expressed by the diffusion-advection differential equation with/without decay term and/or source/sink terms. The fluid carrying the substance is assumed to be incompressible. In three dimensions (3D) the unsteady transport equation is expressed as:

$$\frac{\partial c}{\partial t} = D_x \frac{\partial^2 c}{\partial x^2} + D_y \frac{\partial^2 c}{\partial y^2} + D_z \frac{\partial^2 c}{\partial z^2} - u \frac{\partial c}{\partial x} - v \frac{\partial c}{\partial y} - w \frac{\partial c}{\partial z} - k c + R - S \quad (1)$$

where  $c$  is the concentration,  $c(x, y, z, t)$  by mass ( $\text{kg}/\text{m}^3$ ) at location  $(x, y, z)$ , where  $x$  is the longitudinal or downwind coordinate (m),  $y$  is the lateral or cross wind coordinate (m), and  $z$  is the vertical coordinate (m),  $t$  is time (s);  $D_x$ ,  $D_y$ , and  $D_z$  ( $\text{m}^2/\text{s}$ ) are the diffusion coefficients in the  $x$ ,  $y$ , and  $z$  directions respectively;  $u$ ,  $v$ , and  $w$  (m/s) are the advective velocities in the  $x$ ,  $y$ , and  $z$  directions respectively,  $k$  is the substance decay coefficient (1/s),  $R$  is the source term (due to aerial production of pollutants) ( $\text{kg}/\text{m}^3/\text{s}$ ) and  $S$  is the sink term (due to dry or wet deposition of pollutants) ( $\text{kg}/\text{m}^3/\text{s}$ ).

The governing equation for pollutant transport, Eq. (1), is solved in SUITE-3D numerically by the standard Galerkin Finite Element (FE) method. The details of using the finite element method to solve differential equations can be found in [24], [25], [26], [27] and [28]. In the finite element formulations, the governing equation is written in its weak form. That is, the weighted average of the governing differential equation over the domain of analysis is required to be zero for arbitrary weighting function. Following the standard Galerkin's method, the weighting function is interpreted as variation in the dependent variable which is concentration function). Integration by parts of the integral equation reduces the second order derivative terms (the diffusion terms) to first order derivatives. This puts weaker demands on the required numerical solution and hence the name weak form comes.

In order to approximate the unknown concentration function (required solution) for three dimensional problems the 8-node cubic brick (hexahedron) element is used. The diffusion coefficients and velocities in Eq. (1) are assumed constant within each element but they can vary from element to element to express inhomogeneity. Actually SUITE-3D allows the diffusion coefficients, advection velocities, and all model coefficients to vary in three dimensions and time as functions of  $(x, y, z, t)$ . Substitution of the finite element approximating function of the concentration into the weak form of the governing equation results in an integral equation. This equation is integrated over each element using eight Gaussian quadrature points. The FE model uses the standard Galerkin formulation without upwinding schemes. Integration of the unsteady term is implemented using Crank-Nicolson integration scheme with the option of applying central, or backward or forward difference. The contributions of all element integrations are added together to obtain a global stiffness matrix and forcing right hand side vector, the solution of this matrix system after applying the appropriate boundary conditions represents the finite element approximation of the original differential equation, Eq. (1). The global stiffness matrix is sparse therefore skyline storage is used with an equation solver suitable for skyline matrices.

In this study testing of the numerical finite element code is made using two analytical solutions for 3D unsteady transport differential equation. Several advantages are gained in this way which include (1) making sure that every physical mechanism such as diffusion or advection or decay or source mechanisms is modelled properly, (2) understanding how each mechanism is working and how the different mechanisms are interacting with each other, (3) understanding the role of the boundary conditions of the problem at hand, (4) building a numerical code or model that can be general enough to the maximum extent without being restricted to certain cases in which negligence of some important factors is made such as in Gauss plume models, and (5) understanding the limits of the numerical modelling process through investigation of changes in the model

parameters. In the following, the results are presented for applying the developed FE model to the two test cases that have analytical solutions. One case has 3D unsteady diffusion and advection while the second case has, in addition to diffusion and advection, decay and source terms. This is followed by application of the developed model to air pollution dispersion modeling.

**3. Results and discussion of applying the developed finite element (FE) model:**

**3.1. Problem I: three dimensional unsteady advection and diffusion:**

An exact analytical solution exists for the case in which the transport equation coefficients are constants. For example, when  $D_x = D_y = D_z = 0.5$  and  $u = v = w = 0.5$  while the decay, source, and sink terms are assumed zeros in this case Eq. (1) becomes:

$$\frac{\partial c}{\partial t} = \frac{1}{2} \frac{\partial^2 c}{\partial x^2} + \frac{1}{2} \frac{\partial^2 c}{\partial y^2} + \frac{1}{2} \frac{\partial^2 c}{\partial z^2} - \frac{1}{2} \frac{\partial c}{\partial x} - \frac{1}{2} \frac{\partial c}{\partial y} - \frac{1}{2} \frac{\partial c}{\partial z} \quad (2)$$

The analytical solution is given, Cheng and Zheng (2020), as:

$$c(x, y, z, t) = (e^{-x} + e^{-y} + e^{-z}) e^t \quad (3)$$

The initial condition is taken from Eq. (3) by substituting the time  $t = 0.0$  in the analytical solution, i.e., the initial condition is  $(x, y, z, 0) = (e^{-x} + e^{-y} + e^{-z})$ . A cubic region with  $[0, 1] \times [0, 1] \times [0, 1]$  is considered where the space coordinates and time here could be assumed dimensionless. This is done by scaling the length and time coordinates with characteristic length and time, respectively and assuming any resulting quantity from the non-dimensionalizing process as unity. The boundary conditions for each of the six coordinate planes are obtained from Eq. (3) by substituting  $x = 0, x = 1, y = 0, y = 1, z = 0,$  and  $z = 1$  at each corresponding plane. For example at the plane  $x = 0$  the boundary condition on this plane is taken by substituting  $x = 0$  in Eq. (3) for the concentration function to get:  $c(0, y, z, t) = (1 + e^{-y} + e^{-z}) e^t$ . Central difference is used in all the cases herein to perform the time integration process. In accordance with Cheng and Zheng (2020) a dimensionless time step of 0.01 is selected, and  $11 \times 11 \times 11$  nodes are distributed regularly. This means that 1000 elements are used as shown in Fig. (1), which shows the 3D mesh.

Two types of percentage relative errors are defined here; namely the point wise error (%  $e_p$ ) and the overall or total relative error (%  $e_t$ ). The point wise percentage relative error is defined at any point  $(x, y, z)$  as:

$$\% e_p = \frac{c_{FE} - c_{exact}}{c_{exact}} \times 100 \quad (4)$$

Where  $c_{FE}$  is the calculated concentration by the Finite Element code (SUITE-3D) and  $c_{exact}$  is the concentration form the exact analytical solution. The domain overall or total percentage relative error is defined as:

$$\% e_t = \sqrt{\frac{\sum_{i=1}^n (c_{FE,i} - c_{exact,i})^2}{\sum_{i=1}^n c_{exact,i}^2}} \times 100 \quad (5)$$

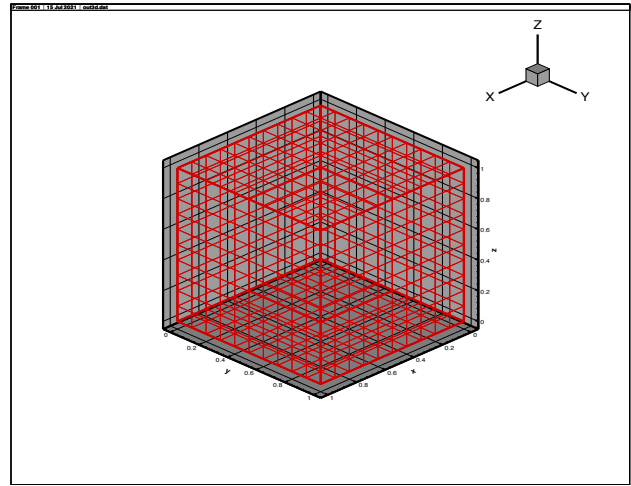


Fig. 1. Mesh of  $11 \times 11 \times 11$  nodes ( $10 \times 10 \times 10$  elements) for problems: I, II and III.

where  $i$  is node number  $i$ , and  $n$  is the total number of nodes over which the summation is carried out.

The volume of the domain is calculated in the SUITE-3D by calculating the volume of each element and summing up over all the whole elements. The exact volume of the unit cubic domain is equal to 1.0 while SUITE-3D calculated volume is 1.000000000000127 resulting in an absolute error of  $10^{-11}$  and a percentage relative error of  $10^{-9}\%$ . These very small error values validate the construction of the element shape functions and their derivatives in 3D in addition to the numerical integration process. After 100 time steps or at dimensionless time,  $t = 1$  it took 22.73 s of CPU time. By comparing SUITE-3D solution with the analytical solution at  $t = 1$ , the maximum point-wise percentage relative error (%  $e_p$ ) is 0.907 % and it is located at the point (0.9, 0.9, 0.9). Figure 2 shows the vertical profile at the centre of the domain, i.e., at (0.5, 0.5, z) of both the SUITE-3D model and the exact solution as given by Eq. (3) where it can be seen that the two profiles are almost identical. SUITE-3D and the analytical model vertical profiles at (0.5, 0.5, z) are also shown in Table 1 where the maximum percentage relative error is 0.85% at (0.5, 0.5, 0.9). The relative errors, along this central vertical line or the region vertical axis, are ranging from 0.82% to 0.85% where this narrow range of the errors shows uniform error distribution. Table 2 and Figure (3) show the lateral central profile at (0.5, y, 0.5) with the same trend as in the previous vertical profile at (0.5, 0.5, z) and with the maximum percentage relative error of 0.85% at (0.5, 0.9, 0.5). Table 3 and Figure (4) show the same trend also for the longitudinal central profile at (x, 0.5, 0.5). Tables (1), (2) and (3) show symmetry, between the three profiles, is preserved in the SUITE-3D model predicted concentrations. This indicates no round-off errors effect. Figures (5), (6), and (7) show 3D plots of the SUITE-3D model predicted concentrations at different dimensionless times where steep gradients of the concentration function could be noticed which is challenging to the FE numerical method.

Table 4 shows comparison between the SUITE-3D model and that of Cheng and Zheng (2020) at selected times of 0.1, 0.3, 0.5, 0.7, and 0.9. The main differences are that [11] use the Element Free Galerkin (IFG) and the Improved Element Free Galerkin (IEFG) methods which employ higher order polynomials (such as splines) for the trial functions. In addition [11] used backward difference for the time integration and they also used 27 Gaussian quadrature points for numerical integrations of the element matrices. It

is clear from Table 4 that the SUITE-3D model results show much less % relative errors (% e<sub>i</sub>) and much less CPU time at all the selected times. This could be largely due to the increase of the number of quadrature points in [11] which are 27 points compared to 8 points in SUITE-3D FE model in addition to them having higher order trial functions associated with element free or meshless methods they used. It is also noted from Table (4) that in SUITE-3D model the % relative error increases very slightly from about 0.5% to 0.6% after which it stays at a constant value of 0.6% indicating nearly uniform errors distribution while in [11] the % relative errors are almost doubled between t = 0.3 and all the subsequent times. At t = 0.9, the % relative error by [11] is 4.5 times that by SUITE-3D model while their CPU time is about 19 times that by SUITE-3D which shows superiority of by SUITE-3D over their model.

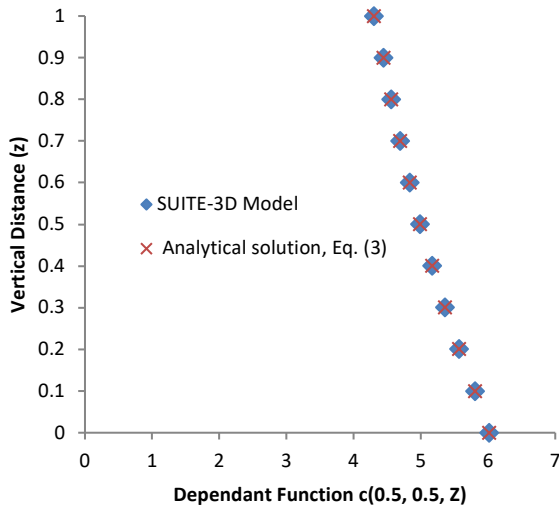


Fig. 2. Problem I, vertical profile of the concentration at  $c(0.5, 0.5, z)$  at dimensionless time,  $t = 1$ .

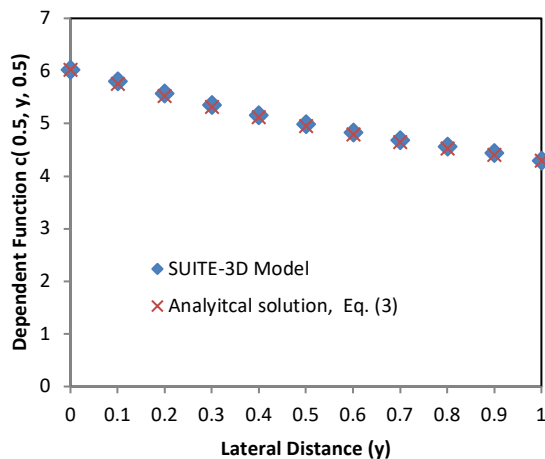


Fig. 3. Problem I, lateral profile of the concentration at  $c(0.5, y, 0.5)$  at dimensionless time,  $t = 1$ .

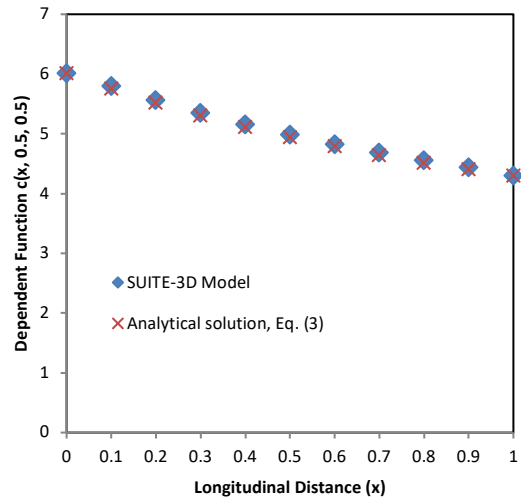


Fig. 4. Problem I, longitudinal profile of the concentration at  $c(x, 0.5, 0.5)$  at dimensionless time,  $t = 1$ .

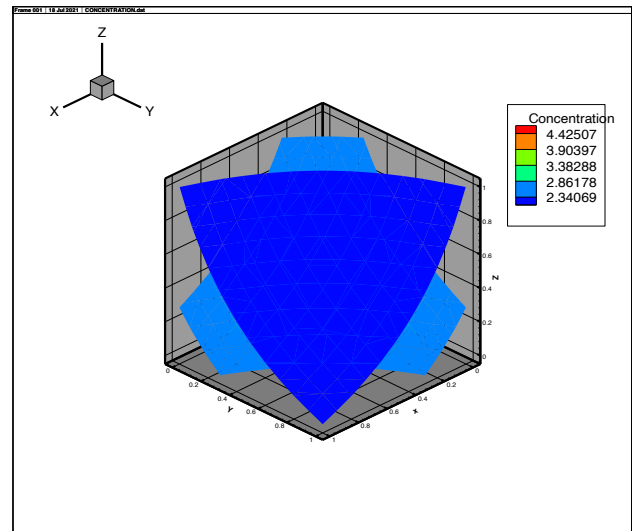


Fig. 5. Problem I: three dimensional plot of SUITE-3D solution at  $t = 0.3$ .

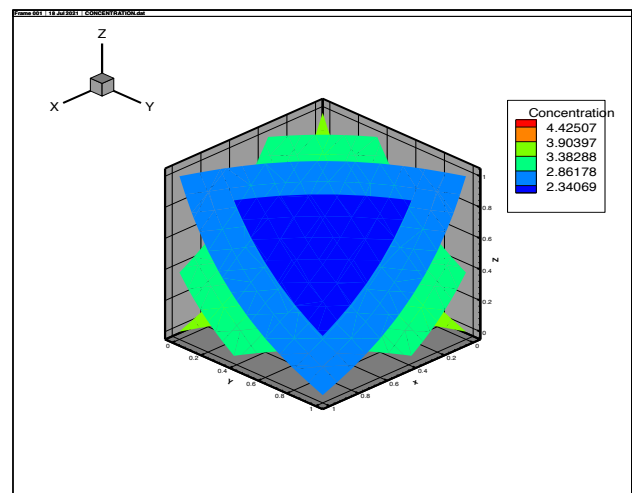


Fig. 6. Problem I: three dimensional plot of SUITE-3D solution at  $t = 0.5$ .

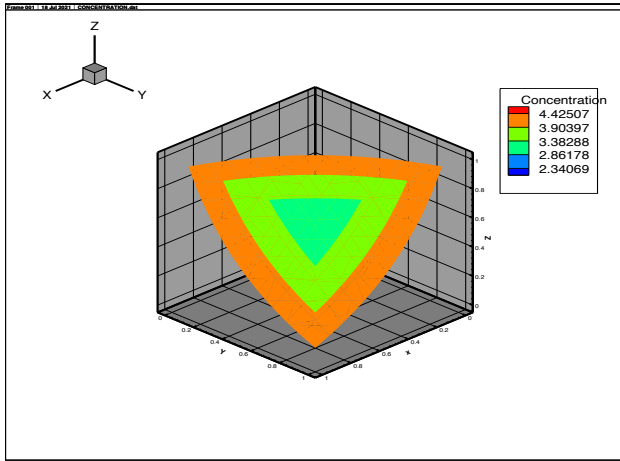


Fig. 7. Problem I: three dimensional plot of SUITE-3D solution at t = 1.0.

**3.2.Problem II: three dimensional unsteady advection and diffusion with decay and source terms**

In this case, in addition to the diffusion and advection terms, decay and source terms are added to represent the full transport differential equation. An example is given by the following equation:

$$\frac{\partial c}{\partial t} = \frac{\partial^2 c}{\partial x^2} + \frac{\partial^2 c}{\partial y^2} + \frac{\partial^2 c}{\partial z^2} - \frac{\partial c}{\partial x} - \frac{\partial c}{\partial y} - \frac{\partial c}{\partial z} - \frac{1}{2} c - \frac{1}{2} e^{(x+y+z-t)} \tag{6}$$

Equation (6) has the following exact solution, Cheng and Zheng (2020), as:

$$c(x, y, z, t) = e^{(x+y+z-t)} \tag{7}$$

It should be noted that Eq. (6) in Cheng and Zheng (2020) was written in another but equivalent form as:

$$\frac{\partial c}{\partial t} = \frac{\partial^2 c}{\partial x^2} + \frac{\partial^2 c}{\partial y^2} + \frac{\partial^2 c}{\partial z^2} - \frac{\partial c}{\partial x} - \frac{\partial c}{\partial y} - \frac{\partial c}{\partial z} - e^{(x+y+z-t)} \tag{8}$$

As was done in Problem I, in running SUITE-3D the initial condition is obtained by letting t = 0 in Eq. (7) while the boundary conditions for each of the six coordinate planes are also obtained from Eq. (7) by substituting x = 0, x = 1, y = 0, y = 1, z = 0, and z = 1 for each corresponding plane. As in the last case a cubic region with [0, 1] × [0, 1] × [0, 1] is considered and is divided into 11 × 11 × 11 nodes distributed regularly, while a time step of 0.01 as before.

**Table 1.** Problem I, the vertical profile of the concentration at c(0.5, 0.5, z) at time = 1.

x	y	z	SUITE-3D Model	Exact solution, Eq. (3)	Absolute error	% relative error
0.5	0.5	0	6.01572	6.01572	0	0.00
0.5	0.5	0.1	5.80436	5.75705	0.04731	0.82
0.5	0.5	0.2	5.56851	5.52298	0.04553	0.82
0.5	0.5	0.3	5.35510	5.31120	0.04390	0.83
0.5	0.5	0.4	5.16197	5.11956	0.04241	0.83
0.5	0.5	0.5	4.98722	4.94616	0.04106	0.83
0.5	0.5	0.6	4.82914	4.78927	0.03987	0.83
0.5	0.5	0.7	4.68614	4.64730	0.03884	0.84
0.5	0.5	0.8	4.55681	4.51885	0.03797	0.84
0.5	0.5	0.9	4.43985	4.40261	0.03724	0.85
0.5	0.5	1	4.29744	4.29744	0	0.00

**Table 2.** Problem I, the lateral Profile of the concentration at c(0.5, y, 0.5) at time = 1.

x	y	z	SUITE-3D Model	Exact Solution, Eq. (3)	Absolute error	% relative error
0.5	0	0.5	6.01572	6.01572	0	0.00
0.5	0.1	0.5	5.80436	5.75705	0.04731	0.82
0.5	0.2	0.5	5.56851	5.52298	0.04553	0.82
0.5	0.3	0.5	5.3551	5.3112	0.04390	0.83
0.5	0.4	0.5	5.16197	5.11956	0.04241	0.83
0.5	0.5	0.5	4.98722	4.94616	0.04106	0.83
0.5	0.6	0.5	4.82914	4.78927	0.03987	0.83
0.5	0.7	0.5	4.68614	4.6473	0.03884	0.84
0.5	0.8	0.5	4.55681	4.51885	0.03797	0.84
0.5	0.9	0.5	4.43985	4.40261	0.03724	0.85
0.5	1	0.5	4.29744	4.29744	0	0.00

**Table 3.** Problem I, the longitudinal profile of the concentration at c(x, 0.5, 0.5) at time = 1.

x	y	z	SUITE-3D Model	Exact solution, Eq. (3)	Absolute error	% relative error
0	0.5	0.5	6.01572	6.01572	0	0.00
0.1	0.5	0.5	5.80436	5.75705	0.04731	0.82
0.2	0.5	0.5	5.56851	5.52298	0.04553	0.82
0.3	0.5	0.5	5.35510	5.31120	0.04390	0.83
0.4	0.5	0.5	5.16197	5.11956	0.04241	0.83

0.5	0.5	0.5	4.98722	4.94616	0.04106	0.83
0.6	0.5	0.5	4.82914	4.78927	0.03987	0.83
0.7	0.5	0.5	4.68614	4.64730	0.03884	0.84
0.8	0.5	0.5	4.55681	4.51885	0.03797	0.84
0.9	0.5	0.5	4.43985	4.40261	0.03724	0.85
1	0.5	0.5	4.29744	4.29744	0	0.00

**Table 4.** Problem I: comparison of the current FE model and Cheng and Zheng model (2020) at various times.

Comparison	Dimensionless Time				
	0.1	0.3	0.5	0.7	0.9
Relative error (%), Cheng and Zheng (2020)	1.2654	2.5893	2.7382	2.7478	2.7483
Relative error (%), SUITE-3D model	0.5288	0.6031	0.6061	0.6062	0.6062
CPU time of EFG (s), Cheng and Zheng (2020)	101.6	176.0	250.5	327.8	395.8
CPU time of IIEFG (s), Cheng and Zheng (2020)	97.2	173.4	240.5	314.9	386.3
CPU time, SUITE-3D model	2.14	6.69	11.33	15.93	20.44

Figure (8) shows excellent match exists between SUITE-3D model predicted concentrations and the exact solution as given by Eq. (7) along the longitudinal axis (x, 0.5, 0.5). It can be seen that the concentration function increases in nonlinear fashion compared to its decreasing trend in Problem I. Figures (9) and (10) show 3D contour plots of SUITE-3D model predicted concentrations at times 0.5 and 1, respectively. Table (5) shows the relative errors are very close between SUITE-3D model and [11] model. The same trend exists between the two models in which the relative error increases from t = 0.3 to t = 0.5 after which it starts to decrease but in a narrow range. The CPU by the SUITE-3D model is very much less than both methods of EFG and IIEFG by [11], i.e., almost hundred times less.

Considering that the methods of [11] employ higher order polynomial trial functions, use 27 Gaussian quadrature

points and have much more CPU time, that shows the superiority of SUITE-3D model. In addition, considering that Problem II has more computational challenge than in Problem I due to the addition of the decay and source terms, it is surprising that the percentage relative errors in [11] are less in Problem II than in Problem I. However, as it is expected, the % relative errors in SUITE-3D model are less in Problem I than in Problem II in conformation with the added level of complexity in Problem II due to addition of the decay and source terms. In summary the preceding results confirm the success of SUITE-3D the unsteady 3D FE model in solving advection-diffusion transport equation with high accuracy and small CPU time. This leads to considering SUITE-3D model to study practical problems such as air dispersion modelling as in the following section. Indeed predicting the concentration of air pollutants is very important for environmental pollution studies.

**Table 5.** Problem II: comparison of the current FE model and Cheng and Zheng model (2020) at various times.

Comparison	Time				
	0.1	0.3	0.5	0.7	0.9
Relative error (%) Cheng and Zheng (2020)	0.6156	0.8093	0.8109	0.8109	0.8109
Relative error (%) SUITE-3D model	0.9800	1.0000	0.9600	0.8900	0.8200
CPU time of EFG (s) Cheng and Zheng (2020)	313.2	816.7	1338.4	1822.8	2325.8
CPU time of IIEFG (s) Cheng and Zheng (2020)	303.9	785.3	1269.3	1763.8	2251.9
CPU time (s) SUITE-3D model	2.37	7.54	12.59	17.50	22.46

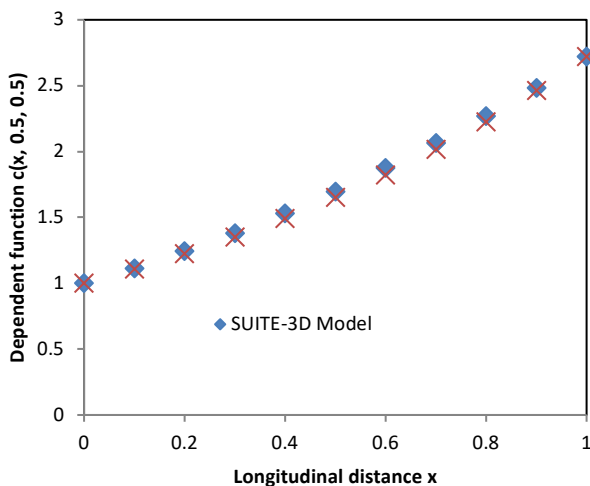


**Fig. 8.** Problem II, longitudinal concentration profile at time = 1.

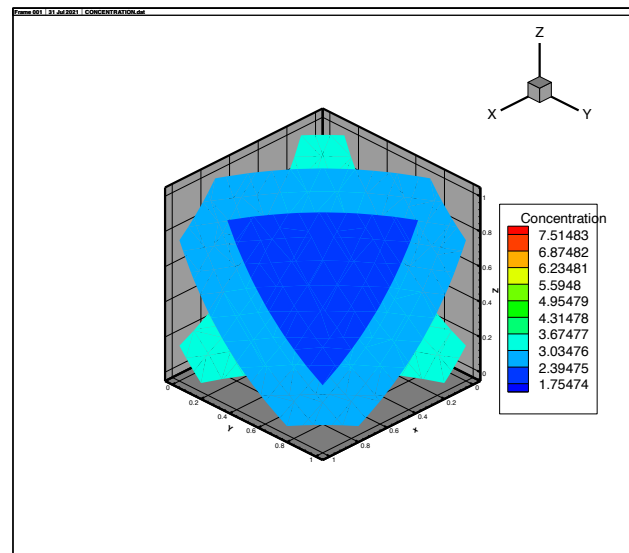


**Fig. 9.** Problem II three dimensional plot of SUITE-3D solution at t = 0.5.

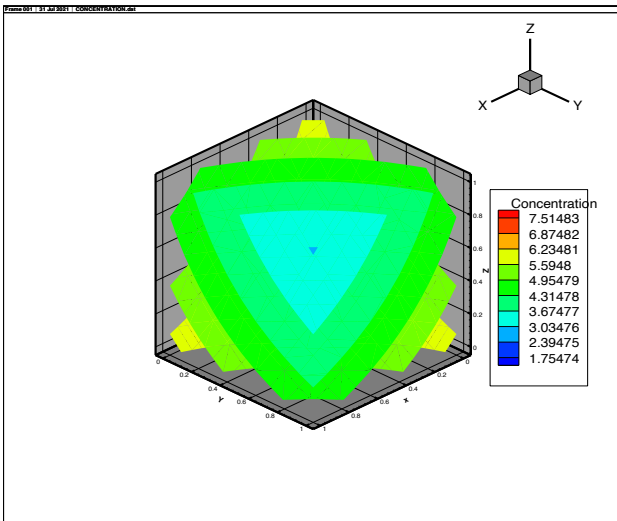


Fig. 10. Problem II three dimensional plot of SUITE-3D solution at t = 1.0.

**3.3. Three dimensional advection and diffusion due to pollution by industrial point source**

In this case, solution of the three dimensional advection and diffusion equation is developed where a point source pollutant is the driving force for concentration dispersion. The pollutant substance is assumed to be non-decaying, and in addition, sources and sinks are assumed vanishing (i.e., k, R, and S are zeros) which reduces Eq. (1) to:

$$\frac{\partial c}{\partial t} = D_x \frac{\partial^2 c}{\partial x^2} + D_y \frac{\partial^2 c}{\partial y^2} + D_z \frac{\partial^2 c}{\partial z^2} - u \frac{\partial c}{\partial x} - v \frac{\partial c}{\partial y} - w \frac{\partial c}{\partial z} \quad (9)$$

Unfortunately when the loading is a pollutant point source, there is no analytical solution to the 3D unsteady advection-diffusion equation as given by Eq. (9). The existing analytical solution exists only under steady, unidirectional flow (usually in the x direction) and without the x diffusion term. Under these conditions, the analytical solution is given by the well-known Gaussian plume model equation. It is given, [29], as:

$$c(x, y, z) = \frac{Q}{2 \pi U_p \sigma_y \sigma_z} e^{\left\{ \frac{-y^2}{2 \sigma_y^2} \right\}} \left[ e^{\left\{ \frac{-(z - H_p)^2}{2 \sigma_z^2} \right\}} + e^{\left\{ \frac{-(z + H_p)^2}{2 \sigma_z^2} \right\}} \right] \quad (10)$$

where Q is the point source rate which is assumed to be continuous and constant in time,  $U_p$  is the wind velocity in the x direction at the height of the stack and  $H_p$  is the stack height (actual stack height plus the plume rise height). All quantities appearing in Eq. (10) are assumed constant with respect to time. The quantities  $\sigma_y$  and  $\sigma_z$  are in m and given as:

$$\sigma_y = \sqrt{2 D_y \frac{x}{u}} \quad \text{and} \quad \sigma_z = \sqrt{2 D_z \frac{x}{u}} \quad (11)$$

In the Gaussian plume equation, Eq. (10), it is assumed that the boundaries (except the boundary at the ground at  $z = 0$ ) are at infinite distance from the pollutant source and the concentrations approach zeros at these boundaries. This constitutes difficulty to compare with numerical models in which the domain is finite. Another difficulty is that for the continuous point source release and infinite boundary domain, true steady conditions will not be reached as the plume front will continue to move in the three directions

indefinitely, however, Eq. (10) assumes steady state conditions.

To overcome these difficulties and to allow for some form of comparison between the 3D unsteady finite element model, SUITE-3D, with finite domain on one hand and the steady infinite domain Gaussian plume model on the other hand, some considerations are taken. These include making sure that the boundary concentrations are equal in both models as much as possible in order to minimize the unsteady differences. This leaves the comparison to be fair in all the interior nodes which are different than the boundary nodes. In this case effects of neglecting the x diffusion term in the Gaussian plume model could be assessed.

A three dimensional domain with length coordinates of 400 m in x, y, and z directions is selected. This selection was made after several trials using different dimensions until the boundary concentrations were found nearly equal between SUITE-3D and the Gaussian plume model as will be shown later. Figure (11) shows the finite element mesh where the elements are cubic bricks (hexahedrons) with length equal to 20.0 m. The mesh is composed of  $21 \times 21 \times 21$  nodes with 8000 total elements. The horizontal diffusion coefficients ( $D_x$  and  $D_y$ ) are assumed equal to  $2.2 \text{ m}^2/\text{s}$  while the vertical diffusion ( $D_z$ ) coefficient is assumed as  $0.5 \text{ m}^2/\text{s}$ . Only velocity in the x direction (u) is considered to be non-zero with an assumed value of 0.2 m/s representing calm wind conditions ( $v = w = 0$ ). At distances of 200 m and 400 m Eq. (11) results in  $\sigma_y$  equal to 66 m and 94 m, respectively while at the same distances  $\sigma_z$  is 32 m and 45 m, respectively.

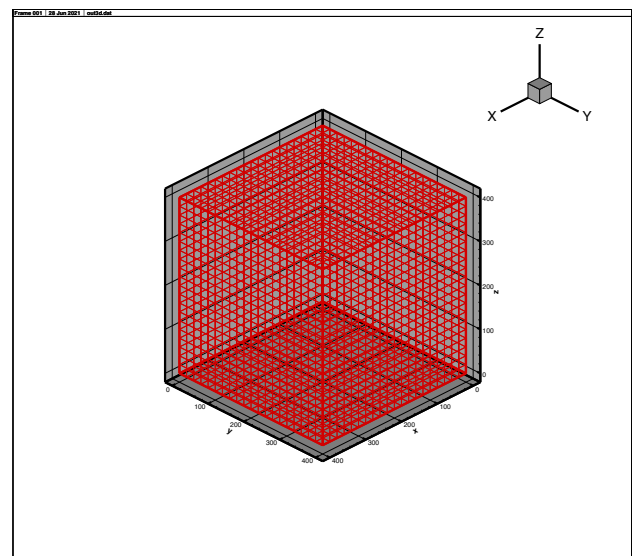


Fig. 11. Mesh of  $11 \times 11 \times 11$  nodes ( $10 \times 10 \times 10$  elements) with element length of 20.0 m.

For stability of the used standard Galerkin's FE scheme it is required that the step or element length  $\Delta x < (2 D_x)/u$ , [27], which for  $D_x = 2.2 \text{ m}^2/\text{s}$  and  $u = 0.2 \text{ m/s}$  results in  $\Delta x < 22 \text{ m}$ . Therefore cubic elements of length equal to 20.0 m satisfy the stability conditions. The point source is located at coordinates (0.0, 200.0, 200.0) (m, m, m) with pollutant load equal to  $0.5 \text{ gm/s}$  (15.768 ton/year). The boundary conditions in SUITE-3D are taken as zero normal derivatives at all boundaries while making sure that no appreciable concentrations are reaching the boundaries. After several numerical trials it is found that the cubic

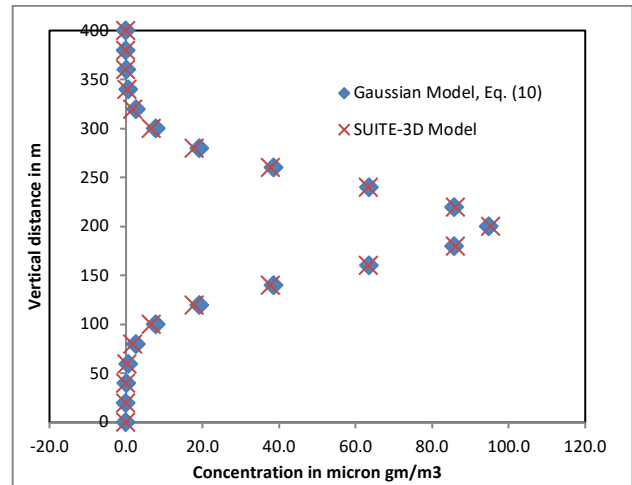
domain with side length of 400 m and at time equal to 2400 s, the predicted concentrations by SUITE-3D and Gaussian dispersion model are nearly equal at the boundaries especially the downstream exit boundary at  $x = 400$  m.

Table (6) and Figure (12) show SUITE-3D and Gaussian plume model vertical concentration profiles, at time 2400 s at the line (400m, 200m, z), are very close especially at the centre at  $z = 200$ m. At (400 m, 200 m, 200 m, 2400 s), the Gaussian model predicts  $94.8 \mu\text{ gm/m}^3$  while SUITE-3D predicts  $95.3 \mu\text{ gm/m}^3$  which is very close. Table (7) and Figure (13) show that SUITE-3D and Gaussian horizontal concentration profile at (400m, y, 200m, 2400s) are very close while some little differences exist at the side boundaries. Because the y diffusion coefficient is higher than the z diffusion coefficient, the concentrations at the y boundaries ( $y = 0$  m and  $y = 400$  m) are higher than those at the z boundaries ( $z = 0$  m and  $z = 400$  m). Symmetry is observed in all SUITE-3D profiles about the centre of the plane  $x = 400$  m confirming model stability and convergence with no round-off error effects. In overall, it is quite clear that at the boundary planes and at time 2400 s the boundary concentrations are very close by both SUITE-3D and the Gaussian plume model which allows for performing comparisons in the interior region.

**Table 6.** Comparisons between predicted concentrations by the FE and Gaussian Plume model at (400, 200, z) at 2400 s.

Vertical Distance (z) in m at $x = 400$ m and $y = 200$ m	SUITE-3D Model Predicted concentrations in $\mu\text{ gm/m}^3$	Gaussian Plume Model Predicted concentrations in $\mu\text{ gm/m}^3$
0	0.0	0.0
20	0.0	0.0
40	0.0	0.2
60	0.3	0.7
80	1.8	2.6
100	6.6	7.8
120	17.9	19.1
140	37.7	38.6
160	63.3	63.6
180	86.1	85.8
200	95.3	94.8
220	86.1	85.8
240	63.3	63.6
260	37.7	38.6
280	17.9	19.1
300	6.6	7.8
320	1.8	2.6
340	0.3	0.7
360	0.0	0.2
380	0.0	0.0
400	0.0	0.0

Table (8) and Figure (14) show the longitudinal concentration profiles by both SUITE-3D and Gaussian plume model along the line (x, 200m, 200m) which is at the plume horizontal or longitudinal axis or centreline; at time 2400 s. It should be noted that at the plane  $x = 0$  which is the plane containing the point source, the concentrations could not be obtained from the Gaussian plume model, Eq. (10), (because  $x = 0$  appears in the denominator of Eq. (10)) and therefore a value could not be given at  $x = 0$  in all the Gaussian longitudinal profiles. One advantage of SUITE-3D model is that the concentrations could be predicted at  $x = 0$  especially the concentration at just the point source itself.



**Fig. 12.** Vertical concentration profiles at the mid plane  $y = 200$  m, the exit plane  $x = 400$  m and at time 2400 s.

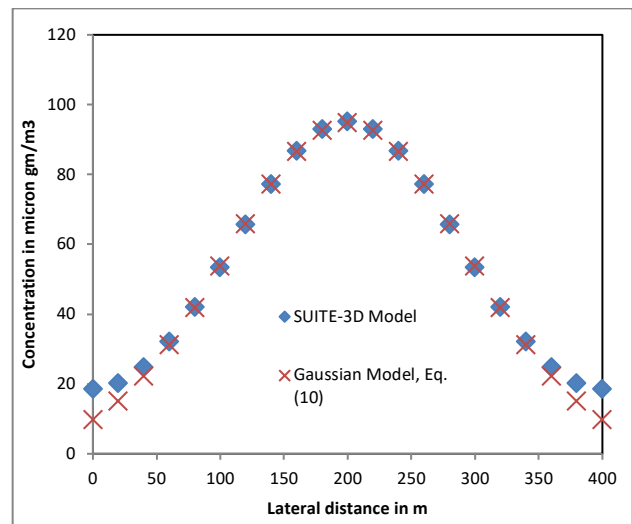


**Fig. 13.** Transverse concentration profiles at the height  $z = 200$  m, the exit plane  $x = 400$  m and at time 2400 s.

**Table 7.** Comparisons between predicted concentrations by the FE and Gaussian Plume model at (400, y, 200) at 2400 s.

Horizontal distance (y) in m at $x = 400$ m and $z = 200$ m	SUITE-3D model concentrations in $\mu\text{ gm/m}^3$	Gaussian plume model concentrations in $\mu\text{ gm/m}^3$
0	18.6	9.8
20	20.1	15
40	24.7	22.1
60	32.1	31.1
80	42	41.8
100	53.5	53.7
120	65.6	65.9
140	77.2	77.3
160	86.7	86.6
180	93	92.7
200	95.3	94.8
220	93	92.7
240	86.7	86.6
260	77.2	77.3
280	65.6	65.9
300	53.5	53.7
320	42	41.8
340	32.1	31.1
360	24.7	22.1
380	20.1	15
400	18.6	9.8

It is noted from Table (8) that SUITE-3D model predicts concentration of about  $2848 \mu\text{ gm/m}^3$  right at the point source which is the maximum concentration value before the pollutant is dispersed away. At a distance 20 m downstream of the source SUITE-3D concentration is -22.5% of the Gaussian plume equation. Further downstream SUITE-3D concentration is higher and the difference increases from about 13% up to 80.6% near the middle and then decreases again toward the downstream end till it reaches 0.4% at the downstream boundary. Figure (14) shows the difference between the two model concentration profiles at the plume horizontal axis which basically could be due to neglecting the x diffusion term in the Gaussian plume model, Eq. (10). Indeed, an 81% and 79% differences at distances of 180 m and 200 m, respectively, from the point source is very significant under-prediction of the Gaussian plume model.

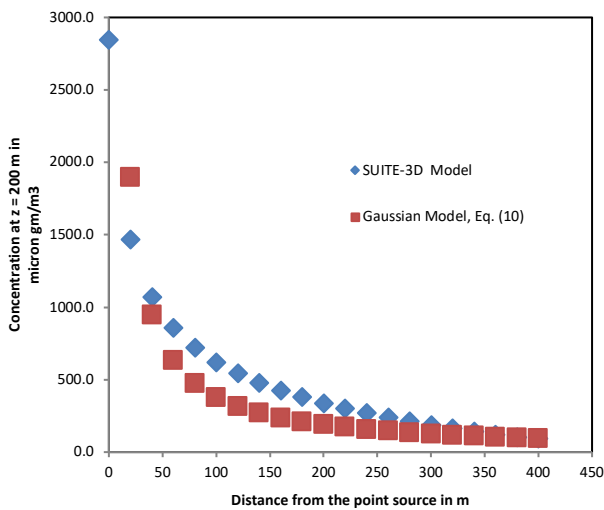


Fig. 14. Longitudinal concentration profiles along the plume horizontal axis (x, 200, 200) and time at 2400 s.

Table (9) and Figure (15) show the longitudinal concentration profile at a height of  $z = 180 \text{ m}$  and  $y = 200 \text{ m}$  and time at 2400 s. It is apparent from Table (9) that SUITE-3D model prediction is about 62% higher than the Gaussian model at just 20 m downstream of the point source, reaches 47% at  $x = 200 \text{ m}$  and it continues to decrease in moving downstream till it reaches 0.3% at  $x = 400 \text{ m}$ . The percentage differences along the whole profile between the two models at  $z = 180 \text{ m}$  is less than those at  $z = 200 \text{ m}$  due to basically decrease in the concentration levels through dispersion. Figure (16) shows the same profile trend at lower level at  $z = 160 \text{ m}$ . Table (10) shows SUITE-3D model concentration starts with about 100% more than the Gaussian model concentration, decreases to about 55% at the middle at  $x = 200 \text{ m}$  and finally reaches -0.4% at the exit plane  $x = 400 \text{ m}$ . Figure (16) shows initial rise of SUITE-3D model concentrations then a decreasing trend. The Gaussian plume model shows initial rise followed by near constant concentration starting from  $x = 100 \text{ m}$  followed by a slight linear decrease in moving toward the boundary exit.

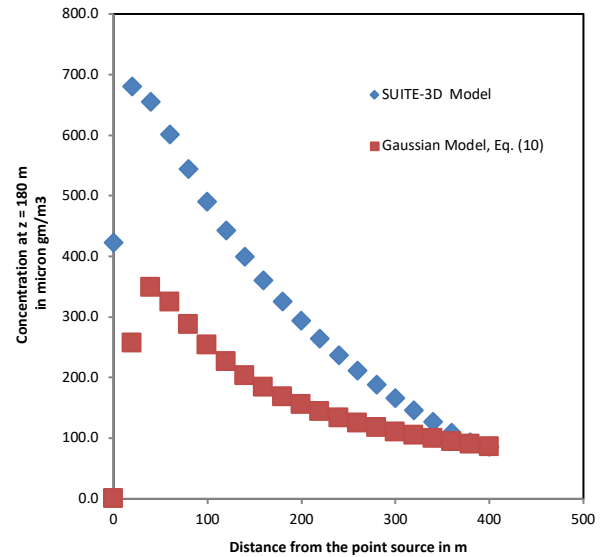


Fig. 15. Longitudinal concentration profiles along the line (x, 200, 180) and time at 2400 s.

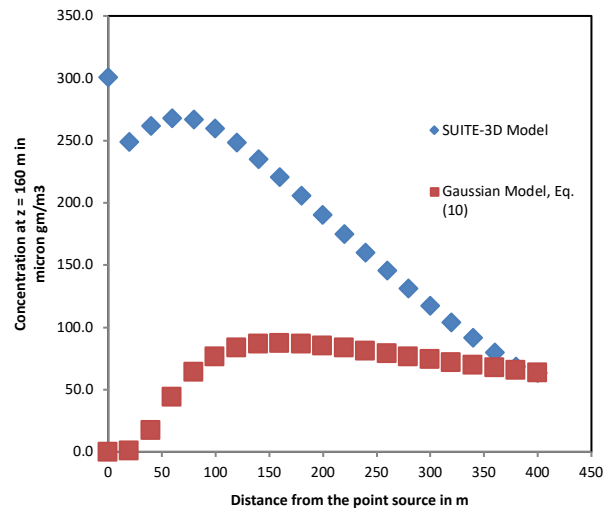


Fig. 16. Longitudinal concentration profiles along the line (x, 200, 160) and time at 2400 s.

It is evident that from the three longitudinal profiles at  $z = 200 \text{ m}$ ,  $180 \text{ m}$ , and  $160 \text{ m}$  that there is significant differences between SUITE-3D and the Gaussian model concentrations (as when using AERMOD) which are primarily due to neglecting the x-diffusion term especially when the velocity is relatively small and calm with  $0.2 \text{ m/s}$ . At such conditions diffusion effects are more dominant than advection effects when the velocity is relatively small under calm wind conditions. As stated before by [19] that the situations of calm conditions have proven to be the most dangerous ones in real-life atmospheric dispersion problems as they are often connected to a stably stratified atmosphere or low-level inversions. For higher velocity values say of the order more than  $1.0 \text{ m/s}$ , advection effects dominate much more than diffusion and the pollutant is transported far away at further distances.

**Table 8.** Comparisons between predicted concentrations by the FE and Gaussian Plume model at (x, 200, 200) at 2400 s.

Longitudinal distance (x) in m at y = 200 m and z = 200 m	SUITE-3D model predicted concentrations in $\mu\text{ gm/m}^3$	Gaussian plume model predicted concentrations in $\mu\text{ gm/m}^3$	Percentage Difference
0	2848.2	NA	NA
20	1469.4	1896.9	-22.5
40	1073.0	948.4	13.1
60	859.7	632.3	36.0
80	721.9	474.2	52.2
100	622.1	379.4	64.0
120	544.4	316.1	72.2
140	480.9	271.0	77.5
160	427.2	237.1	80.2
180	380.7	210.8	80.6
200	339.7	189.7	79.1
220	303.1	172.4	75.8
240	270.0	158.1	70.8
260	239.9	145.9	64.4
280	212.2	135.5	56.6
300	186.8	126.5	47.7
320	163.4	118.6	37.8
340	141.7	111.6	27.0
360	121.8	105.4	15.6
380	103.8	99.8	3.9
400	95.3	94.8	0.4

**Table 9.** Comparisons between predicted concentrations by the FE and Gaussian Plume model at (x, 200, 180) at 2400 s.

Longitudinal distance (x) in m at y = 200 m and z = 180 m	SUITE-3D model predicted concentrations in $\mu\text{ gm/m}^3$	Gaussian plume model predicted concentrations in $\mu\text{ gm/m}^3$	Percentage Difference
0	422.8	NA	NA
20	680.5	256.7	62.3
40	655.5	348.9	46.8
60	601.3	324.6	46.0
80	544.0	287.6	47.1
100	490.7	254.3	48.2
120	442.7	226.5	48.8
140	399.6	203.6	49.0
160	360.8	184.7	48.8
180	325.6	168.8	48.2
200	293.5	155.3	47.1
220	264.0	143.8	45.5
240	236.9	133.8	43.5
260	211.7	125.1	40.9
280	188.2	117.5	37.6
300	166.4	110.7	33.5
320	146.1	104.6	28.4
340	127.1	99.2	22.0
360	109.6	94.3	14.0
380	93.6	89.9	4.0
400	86.1	85.8	0.3

**Table 10.** Comparisons between predicted concentrations by the FE and Gaussian Plume model at (x, 200, 160) at 2400 s.

Longitudinal distance (x) in m at y = 200 m and z = 160 m	SUITE-3D model predicted concentrations in $\mu\text{ gm/m}^3$	Gaussian plume model predicted concentrations in $\mu\text{ gm/m}^3$	Percentage Difference
0.0	301.0	NA	NA
20.0	248.8	0.6	99.7
40.0	261.7	17.4	93.4
60.0	268.1	43.9	83.6
80.0	266.8	64.2	75.9
100.0	259.6	76.6	70.5
120.0	248.6	83.3	66.5
140.0	235.3	86.4	63.3
160.0	220.8	87.2	60.5

180.0	205.7	86.6	57.9
200.0	190.4	85.2	55.2
220.0	175.2	83.3	52.4
240.0	160.2	81.2	49.3
260.0	145.6	78.9	45.8
280.0	131.3	76.5	41.7
300.0	117.6	74.2	36.9
320.0	104.3	71.9	31.1
340.0	91.7	69.7	24.0
360.0	79.7	67.6	15.2
380.0	68.6	65.5	4.5
400.0	63.3	63.6	-0.4

Figures from (17) to (19) show 3D, plan, and side view plots of SUITE-3D model predicted concentrations at 1800 s (30 min) while Figures from (20) to (22) show the same graph types but at 2400 s (40 min). Figures (17) and (20) show the typical plume bell shape of the pollutant concentration predicted by SUITE-3D model as expected.

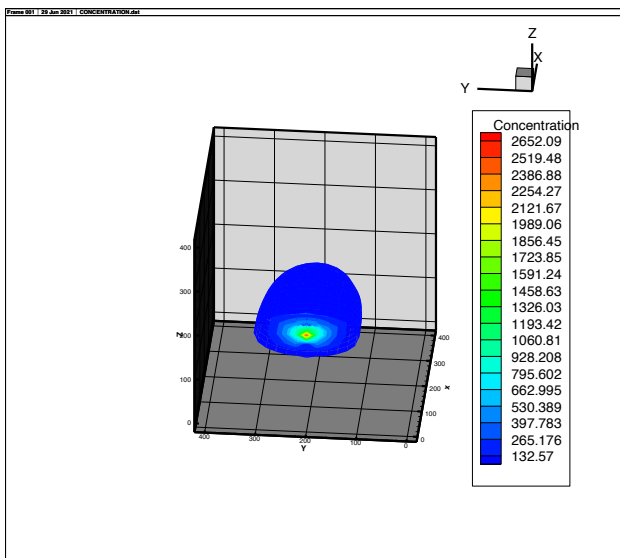


Fig. 17. 3D plot of the concentration contours by SUITE-3D due to point source at 30 minutes (1800 secs).

Future developments of SUITE-3D include using the 3D velocities-pressure model (already developed, [24]) to predict the 3D unsteady flow and pressure field. This will allow investigations of plume rise, terrain effects and effects of buildings and obstacles. Also SUITE-3D can be used in investigation of temperature effects with its links to the pressure and the velocity fields. For large scale problems where the domain could be in the order of several kilometres there are two-dimensional model versions which is 2D vertical (SUITE-2DV) and the other is 2D horizontal (SUITE-2DH).

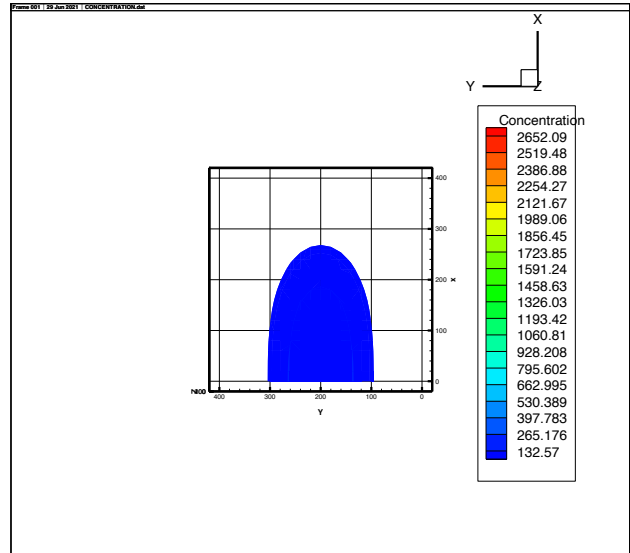


Fig. 18. Plan view (x-y plane) of the concentration by SUITE-3D due to point source at 30 minutes (1800 secs).

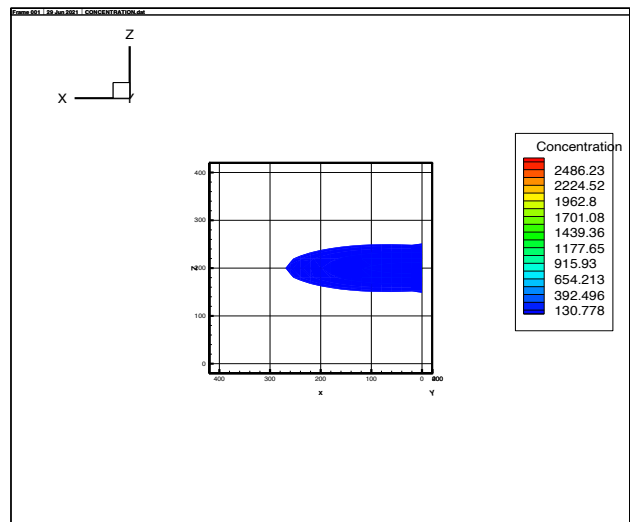


Fig. 19. Side view (x-z plane) of the concentration by SUITE-3D due to point source at 30 minutes (1800 secs).

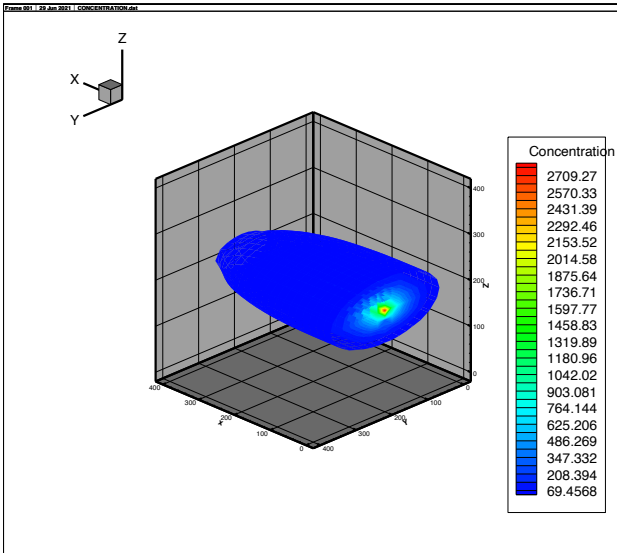


Fig. 20. 3D plot of the concentration contours by SUITE-3D due to point source at 40 minutes (2400 secs).

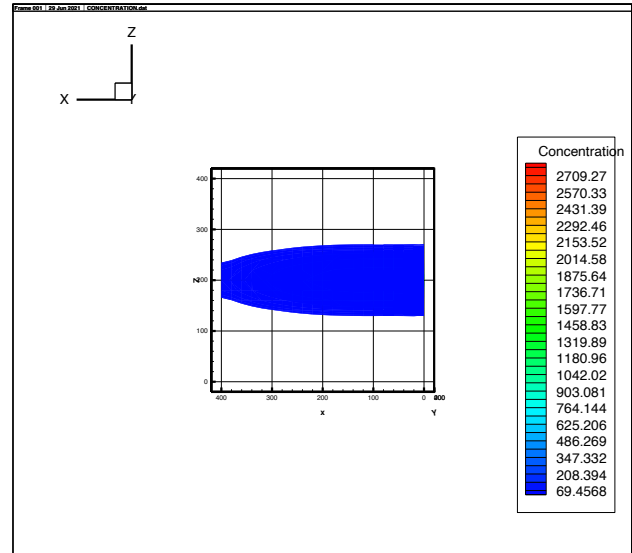


Fig. 22. Side view (x-z plane) of the concentration contours by SUITE-3D due to point source at 40 minutes (2400 secs).

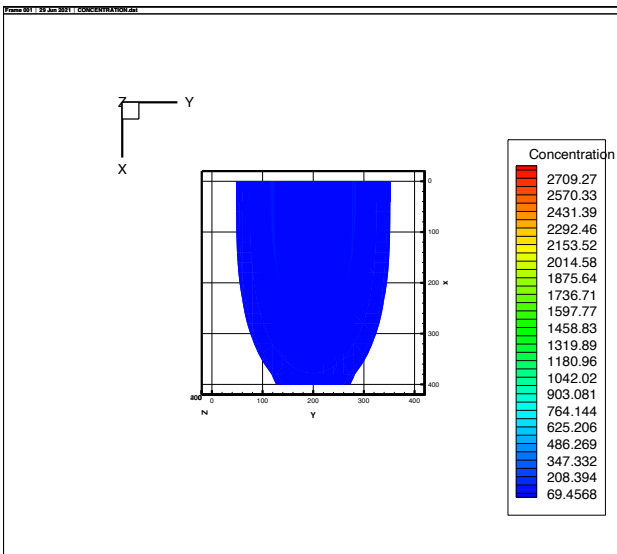


Fig. 21. Plan view (x-y plane) of the concentration contours by SUITE-3D due to point source at 40 minutes (2400 secs).

#### 4. Conclusions

The developed three dimensional unsteady Finite Element model, SUITE-3D, succeeded in solving the three-dimensional unsteady advection-diffusion transport equation. The percentage relative errors in this case are less than 0.61%. For the full transport equation in which decay and source terms exist in addition to the advection and diffusion terms, the percentage relative errors in this case are less than 1.0%. The developed SUITE-3D model showed better accuracy (less % relative errors) and less CPU times when compared with the Cheng and Zheng (2020) Element Free Galerkin (IFG) and the Improved Element Free Galerkin methods. When the developed SUITE-3D model is applied to point source air pollution, the FE model showed concentration under-prediction by up to 81% results in when using Gaussian plume equation under calm wind condition with velocity of 0.2 m/s. This proves that Gaussian models such as AERMOD provide poor results in situations with low wind speeds, where the three-dimensional diffusion is significant. SUITE-3D model was shown to be able to simulate the typical plume bell shape.

This is an Open Access article distributed under the terms of the Creative Commons Attribution License.



#### References

- Hafez, Y.I. and El-Sayed, Awad (2016). Finite Element Modeling of Radon Distribution in Natural Soils of Different Geophysical Regions, Cogent Physics Journal, Vol.3, Issue, 1, 2016.
- Hafez, Y.I., (2022). Understanding Radon (<sup>222</sup>Rn) Transport in One and Multi-layer Soils Using Analytical and Finite Element Modeling, Journal of Hydrology, Volume 610, July 2022, 127803 <https://doi.org/10.1016/j.jhydrol.2022.127803>
- Svoboda, Z., (2000). "The convective-diffusion equation and its use in building physics", International Journal on Architectural Science, Volume 1, Number 2, p. 68-79, 2000.
- Talaa A.M., Hafez, Y.I., Rashad, R.M., and Abdallah, E., (2002). "Prediction of Heat and Mass Transfer Affecting Open Channels Environment" Journal of Environmental Science, Ain Shams University Vol 4, No. 3, June 2002.
- Jha, B.K., Neeru Adlakh, N. and Mehta, M. N., (2012). "Analytic Solution of Two Dimensional Advection Diffusion Equation Arising In Cytosolic Calcium Concentration Distribution", International Mathematical Forum, Vol. 7, 2012, no. 3, 135 – 144.
- Issakhov, A., and Zhandaulet, Y. (2019). Numerical simulation of thermal pollution zones' formations in the water environment from the activities of the power plant. Engineering Applications of Computational Fluid Mechanics, 13(1), 279–299. <https://doi.org/10.1080/19942060.2019.1584126>
- Issakhov, A., and Zhandaulet, Y. (2020). Numerical study of technogenic thermal pollution zones' formations in the water environment from the activities of the power plant. Environmental Modeling & Assessment, 25(2), 203–218. <https://doi.org/10.1007/s10666-019-09668-8>
- Madiraju, S.V.H.; Kumar, A. (2021). Development of a Line Source Dispersion Model for Gaseous Pollutants by Incorporating Wind Shear near the Ground under Stable Atmospheric Conditions.

- Environ. Sci. Proc. 2021, 4, 17. <https://doi.org/10.3390/ecas2020-08154>
9. Gupta, M.M., and Zhang, J., (2000). "High accuracy multigrid solution of the 3D convection-diffusion equation", *Applied Mathematics and Computation* 113 (2000) 249-274.
  10. Saqib, M., Hasnain, S., and Mashat, D.S., (2017). "Computational solutions of three-dimensional advection-diffusion equation using fourth order time efficient alternating direction implicit scheme", *AIP Advances* 7, 085306 (2017); <https://doi.org/10.1063/1.4996341>
  11. Cheng, H. and Zheng, G., (2020). Analyzing 3D Advection-Diffusion Problems by Using the Improved Element-Free Galerkin Method, *Hindawi, Mathematical Problems in Engineering* Volume 2020, Article ID 4317538, 13 pages, <https://doi.org/10.1155/2020/4317538>
  12. Issakhov, A., and Baitureyeva, A. (2019). Modeling of a passive scalar transport from thermal power plants to atmospheric boundary layer. *International Journal of Environmental Science and Technology*, 16(8), 4375–4392. <https://doi.org/10.1007/s13762-019-02273-y>
  13. Issakhov, A., Omarova, P., & Issakhov, A. (2020a). Numerical study of thermal influence to pollutant dispersion in the idealized urban street road. *Air Quality, Atmosphere & Health*, <https://doi.org/10.1007/s11869-020-00856-0>
  14. Issakhov, A.; Alimbek, A. and Issakhov, A. (2020b) A numerical study for the assessment of air pollutant dispersion with chemical reactions from a thermal power plant, *Engineering Applications of Computational Fluid Mechanics*, 14:1, 1035-1061, DOI: 10.1080/19942060.2020.1800515
  15. Issakhov, A., and Omarova, P. (2020). Numerical simulation of pollutant dispersion in the residential areas with continuous grass barriers. *International Journal of Environmental Science and Technology*, 17(1), 525–540. <https://doi.org/10.1007/s13762-019-02517-x>
  16. Daly, A. and P. Zannetti. (2007). *Air Pollution Modeling – An Overview*. Chapter 2 of *AMBIENT AIR POLLUTION* (P. Zannetti, D. Al-Ajmi, and S. Al-Rashied, Editors). Published by The Arab School for Science and Technology (ASST) (<http://www.arabschool.org.sy>) and The EnviroComp Institute (<http://www.envirocomp.org/>).
  17. Leclossy, A., Molnár, F., Izsák, F., Havasi, A., Lagzi, I., and Mészáros, R. (2014) "Dispersion modeling of air pollutants in the atmosphere: a review", *Cent. Eur. J. Geosci.* • 6(3) • 2014 • 257-278 DOI: 10.2478/s13533-012-0188-6
  18. Karroum, K., Lin, Y., Chiang, Y.-Y., Ben Maissa, Y., El Haziti, M., Sokolov, A. and Delbarre, H. (2020). "A Review of Air Quality Modeling", *M. APAN-Journal of Metrology Society of India* (June 2020) 35(2):287–300 <https://doi.org/10.1007/s12647-020-00371-8>
  19. Sharan, M. and Gopalakrishnan, S. G., (1991) Bhopal gas accident: a numerical simulation of the gas dispersion event, *Environ. Model. Softw.*, 12, 1997, 135–141
  20. Anikender Kumar, P. Goyal. (2014). Air Quality Prediction of PM10 through an Analytical Dispersion Model for Delhi. *Aerosol and Air Quality Research*, 14: 1487–1499, 2014 Copyright © Taiwan Association for Aerosol Research ISSN: 1680-8584 print / 2071-1409 online doi: 10.4209/aaqr.2013.07.0236
  21. Katika, K., and Karuchit, S., (2012). "Estimation of Urban Air Pollutant Levels using AERMOD: A Case Study in Nakhon Ratchasima, Thailand." *IOP Conf. Ser.: Earth Environ. Sci.* 164 012024
  22. Joneidi, N., Rashidi, Y., Atabi, F., and Broomandi, P. (2018). "Modeling of Air Pollutants' Dispersion by Means of CALMET/CALPUFF (Case Study: District 7 in Tehran city)" *Pollution*, 4(2): 349-357, Spring 2018 DOI: 10.22059/poll.2018.243144.328 Print ISSN: 2383-451X Online ISSN: 2383-4501 Web Page: <https://jpoll.ut.ac.ir>, Email: [jpoll@ut.ac.ir](mailto:jpoll@ut.ac.ir)
  23. Xie, L., Xu, Q., and He, R. (2021). "Atmospheric Pollution Impact Assessment of Brick and Tile Industry: A Case Study of Xinmi City in Zhengzhou, China.", *Sustainability*, 2021, 13, 2414. <https://doi.org/10.3390/su13042414>
  24. Hafez Y.I., (1995) "A k-ε Turbulence Model for Predicting the Three-Dimensional Velocity Field and Boundary Shear in Open and Closed Channels", Ph.D. Dissertation, Civil Engineering Department, Colorado State University, Fort Collins, Colorado, USA, 1995.
  25. Molinas A., and Hafez Y. I., (2002). "Finite Element Surface Model for Flow Around Vertical Wall Abutments", *Journal of Fluids and Structures*, Academic Press, Vol. 14, No. 5, July 2000, pp. 711-733.
  26. Elbalasy, A.M., Hafez Y.I., and Saad, B.M., (2006) "2D Hydrodynamic Model for Predicting Eddy Fields", 1<sup>st</sup> International Conference on Advances in Engineering and Technology, Entebbe, Uganda
  27. Thompson, E. G., (2005). "Introduction to the finite element method, theory, programming, and applications", (5th ed.). Hoboken, NJ: John Wiley & Sons.
  28. Hafez Y.I., (2017). "A Two-Dimensional Finite Element Channel/Lake Flood Model; Case Study of Edko Drain/Lake, Egypt", *Art Human Open Acc. J* 1(2): 00009. DOI: 10.15406/ahoaj.2017.01.00009
  29. Turner, D.B. (1994). *Workbook of Atmospheric Dispersion Estimates: An Introduction to Dispersion Modeling*. 2<sup>nd</sup> Ed. CRC Press, London. ISBN 1 56670 023 X.